Seismocardiography and Echocardiography: The Correlation in the Systolic Complex

Kolind, Christoffer Mejling; Tange, Alberte Bjerre; Sten, Sandra Toft; Sonne, Maria Mathilde Sauer; Agam, Ahmad; Søgaard, Peter; Schmidt, Samuel

Published in:
Biomedical Physics & Engineering Express

DOI (link to publication from Publisher):
10.1088/2057-1976/ad6a67

Publication date:
2024

Document Version
Publisher's PDF, also known as Version of record

Seismocardiography and echocardiography: the correlation in the systolic complex

IOP Publishing Biomed. Phys. Eng. Express 10 (2024) 055025 https://doi.org/10.1088/2057-1976/ad6a67

Biomedical Physics & Engineering Express

RECEIVED
31 May 2024

REVISED
21 July 2024

ACCEPTED FOR PUBLICATION
2 August 2024

PUBLISHED
13 August 2024

PAPER

Seismocardiography and echocardiography: the correlation in the systolic complex

Christoffer Mejling Kolind[1,*], **Alberte Bjerre Tange**[1,*], **Sandra Toft Sten**[1,*], **Maria Mathilde Sauer Sonne**[1,*], **Ahmad Agam**[1], **Peter Søgaard**[2] and **Samuel Schmidt**[3]

[1] Faculty of Medicine, Aalborg University, Aalborg, Denmark
[2] Department of Cardiology, Aalborg University Hospital, Aalborg, Denmark
[3] Department of Health Science and Technology, Aalborg University, Aalborg, Denmark
[*] Participated equally to the preparation of the article.

E-mail: ckolind20@student.aau.dk

Keywords: echocardiography, seismocardiography, systolic variables, non-invasive, cardiology, preload

Supplementary material for this article is available online

Abstract

Aim. This study aimed to investigate the correlation between seismocardiographic and echocardiographic systolic variables and whether a decrease in preload could be detected by the seismocardiography (SCG). *Methods*. This study included a total of 34 subjects. SCG and electrocardiography were recorded simultaneously followed by echocardiography (echo) in both supine and 30° head-up tilted position. The SCG signals was segmented into individual heartbeats and systolic fiducial points were defined using a detection algorithm. Statistical analysis included correlation coefficient calculations and paired sample tests. *Results*. SCG was able to measure a decrease in preload by almost all of the examined systolic SCG variables. It was possible to correlate certain echo variables to SCG time intervals, amplitudes, and peak to peak intervals. Also, changes between supineand tilted position of some SCG variables were possible to correlate to changes in echo variables. LVET, IVCT, S', strain, SR, SV, and LVEF were significantly correlated to relevant SCG variables. *Conclusion*. This study showed a moderate correlation, between systolic echo and systolic SCG variables. Additionally, systolic SCG variables were able to detect a decrease in preload.

Introduction

In 2019 cardiovascular diseases represented 32% of global deaths, which makes it the leading cause of deaths worldwide [1]. In the United States, the costs of heart failure are almost 31 billion dollars annually [2]. Currently, electrocardiography (ECG) and echocardiography (echo) are some of the most applied non-invasive point-of-care diagnostic methods, of cardiovascular diseases [3, 4]. Echo is a time-consuming examination that requires training and special staff to provide reliable data [5]. Moreover, there is an observer variability even in the hands of experienced operators [6].

Prevalent cases of cardiovascular diseases in the US have almost doubled during the past two decades [7]. As a consequence, the number of echo exams has increased accordingly with the number of referrals for suspected heart diseases [8, 9]. For this reason, it would be relevant to implement seismocardiography (SCG) as it offers potential practical advantages to examine the hemodynamic and mechanical performance. SCG could be a fast and easily manageable supplement to echo. This could potentially reduce examining waiting times, inter-observer variability and have economic advantages.

SCG is a potential non-invasive measure of cardiac function. It uses an accelerometer that measures vibrations from the chest, produced by the beating heart, valve movements, and blood flow. The use of an accelerometer as a tool for measuring cardiac performance and health status has been improved since Patrick Mounsey reported one of the earliest SCG measurements in 1957 [10, 11]. The seismocardiogram displays different amplitude deflections, including a low-frequency wave in atrial systole, a high-frequency wave in ventricular systole, a second wave in early ventricular filling and some relatively high frequency

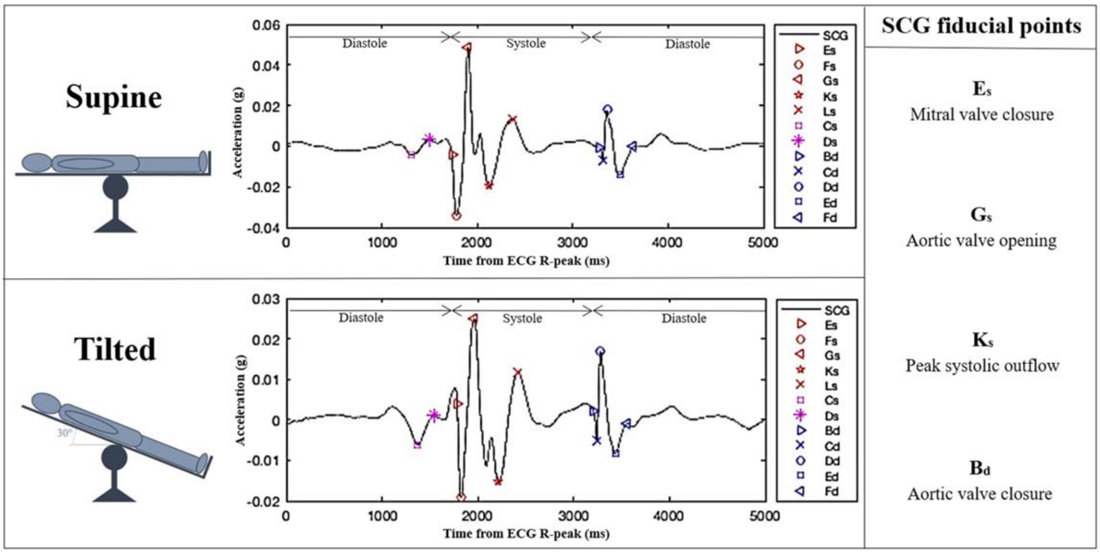

Figure 1. SCG data were recorded in a supine- and a tilted position. The seismocardiograms display the mean curve from subject number nine. Fiducial points of SCG were placed by an algorithm, representing cardiac events as seen in the right column.

waves similar to the heart sounds S1 and S2 [12]. It is considered that SCG signals are produced by mechanical processes including myocardial contraction, valve opening and closing, and hemodynamics [12, 13]. SCG can be acquired at high frequency, stored digitally, and may supplement auscultation.

The correlation between SCG and cardiac function is not fully understood. The findings in the literature are characterized by a lack of consensus on the management, signal processing, and analysis of the SCG [12]. Furthermore, SCG has shown an extensive inter-individual variation, and even more considerable variations are observed in patients with cardiac diseases such as heart failure and aortic stenosis [12, 14]. Even though, as stated in the literature SCG has shown promising usability in the detection of several pathological cardiovascular conditions [15–17]. For example the study by Johnson *et al* [15] indicates that the changes in SCG has promising usability in the detection of coronary artery disease and reduced left ventricular function.

A study by Sørensen *et al* [18] defined fiducial points based on a correlation between SCG deflections and physiological cardiac events displayed on echo. A study by Agam *et al* [19] has demonstrated a correlation between echo variables and SCG in the diastole, using diastolic SCG fiducial points defined by Sørensen *et al* [18]. By investigating the correlation in the systolic function with echo and the preload sensitivity of SCG in the systole, it might be possible to contribute to an enhanced understanding of the diagnostic value of SCG.

The golden standard for evaluation of the systolic function is an echo examination, both in the general assessment of the overall heart function and in follow-up examinations of patients with heart diseases [20]. Systolic dysfunction is a measure of several pathological effects of the heart [21], which substantiates the physiological relevance of investigating the systolic complex in SCG. Aortic stenosis is an example of a pathological condition that impacts the systole. A clinical sign is a systolic murmur detected during auscultation. The current monitoring and quantification of the stenosis requires echo or MRI. The SCG could potentially make the monitoring possible at home or in general practice.

This study aimed to investigate a potential correlation between systolic variables of SCG and echo. Additionally, it was aimed to investigate if a decrease in preload, in 30° head-up tilted position, would be detected by SCG.

Methods

This study included 45 healthy subjects where ECG, SCG and echo data were obtained in both supine and 30° head-up tilted position, as illustrated in figure 1. SCG and ECG were recorded simultaneously and afterwards, an echo was obtained. All the SCG and echo data were analyzed, focusing on the systolic complex.

The data in this study is extracted from the same echo's, ECG's, and SCG's that Sørensen *et al* [18] and Agam *et al* [19] also extracted data from. The experimental protocol was approved by The Scientific Ethical Committee of Northern Jutland (N-20120069). Furthermore, informed written consent was gathered from each subject in advance of the participation and publication. The research was conducted in accordance with the principles embodied in the Declaration of Helsinki and in accordance with local statutory requirements.

Study population

To gather subjects, posters were distributed both at Aalborg University (Aalborg, Denmark) and at local

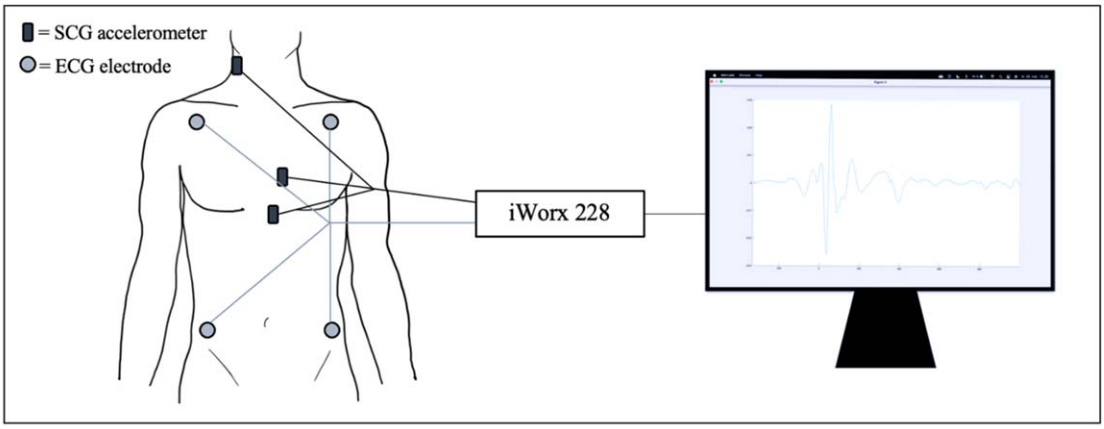

Figure 2. Illustration of the experimental setup including the placement of the SCG accelerometers and the ECG electrodes.

supermarkets. 45 healthy subjects without any known cardiovascular diseases volunteered. The subjects included 17 females and 17 males aged 20–80 years. Subjects diagnosed with any cardiovascular disease, any use of cardiac-related medication or devices, and/or any type of inability to collaborate were excluded.

Experimental design

Demographic data were collected from each subject including height, weight, age, and sex. The subjects were positioned on the back in a supine position, before the attachment of ECG electrodes and SCG accelerometers. Three accelerometers (model 1521, Silicon Designs) were each placed in a 3D-printed plastic housing (19 mm wide, 21 mm long, and 11 mm high, weighing 5 grams) and were attached to the skin using double adhesive tape. One accelerometer was placed respectively at the xiphoid process, one at the left 4 th intercostal space, and one at the right carotid artery, as seen in figure 2. All accelerometers were single-access accelerometers measuring the dorsoventral axis (the *z*-axis). The further analysis of this study only included SCG data recorded at the xiphoid process. To perform the ECG four electrodes were placed on respectively the right and left shoulder and on the right and left iliac crest. The ECG electrodes and accelerometers were connected to an iWorx 228 data acquisition system. The signal was sampled at 5000 Hz using LabScribe software.

Immediately after collecting data from ECG and SCG, the echo was performed with the subjects lying on their side. The Vivid E9 (GE Healthcare, Milwaukee) was used to record the ultrasound images and ECG with electrodes corresponding to the ECG recorded with iWorx 228. The echo was recorded using the following setups: Pulsed Wave Tissue Doppler Imaging (PW TDI) of the lateral mitral annulus and respectively apical two, three and four chamber views. The echo data were assessed manually using the program Viewpoint. All examinations were performed in a supine position and afterwards repeated in a 30° head-up tilted position, to decrease cardiac preload. Great care was taken to ensure that the seismocardiographic and echocardiographic recordings were obtained at identical heart rates to ensure comparable timing. Due to the positioning of the patient during echocardiography and the interference caused by the echo-probe the two measurements are performed in continuation and not simultaneously.

Signal processing

The program MATLAB (Mathworks, USA) was used to process the ECG and SCG data recorded by iWorx 228. The data were recorded continuously during the experiment, and the intervals for respectively supine and tilted position were chosen for the analysis, based on visual inspection whereby intervals without noise contamination were selected. After processing data, different numbers of heartbeats for each subject were able to be detected and thereby included in the data.

A duration-dependent hidden Markow Model (DHMM) described by Schmidt *et al* [22] was used to segment the individual heartbeats. Before the segmentation with the DHMM, the SCG output was high pass filtered (>15 Hz) since the model initially was developed to segment heart sounds. Following the segmentation, the entire SCG-signal of each heartbeat was analysed in MATLAB.

The onset of the first heart sound defined the onset of the systole and the second heart sound the onset of the diastole. To avoid an exchange of the systole and diastole, DHMM segmentation was compared to the ECG signal, and no cases of exchanged values were detected.

The systolic and diastolic segments were aligned and averaged to produce a low noise mean SCG beat for each subject in each position as described by Sørensen *et al* [18]. While some studies choose to low-pass filter the SCG-signal to suppress the components of the SCG signals above 20 to 40 Hz, we chose not to filter to avoid smearing of the fiducial points, thus ensuring more prominant fiducial points. By utilizing

Table 1. The division of the systolic SCG variables into three periods.

Division of the systole				
Period	Amplitudes	Amplitude intervals	Time intervals	
Early systole	F_s	F_s to G_s	E_s to G_s	
	G_s		E_s to F_s	
			F_s to G_s	
Late systole	K_s	G_s to K_s	G_s to K_s	G_s to B_d
	L_s	L_s to K_s	G_s to L_s	K_s to B_d
	B_d		K_s to L_s	L_s to B_d
Entire systole			E_s to B_d	E_s to L_s
			F_s to B_d	F_s to K_s
			E_s to K_s	F_s to L_s

a costume-developed fiducial point detection algorithm the systolic fiducial points E_s, F_s, G_s, K_s, L_s and B_d were identified as by Sørerensen *et al* [18] were identified. In order to validate the fiducial points, they were manually corrected in MATLAB (Mathworks, USA) if a point were not placed equivalent according to the study by Sørensen *et al* [18]. The mean SCG curves with the fiducial points are seen in Supplementary Material 3, where corrected and excluded curves are marked.

Systolic seismocardiographic variables

The parameters included in the study were based on the fiducial points detected by the algorithm by Sørensen *et al* [18], and the systolic time interval was defined as the closure of the mitral valve (E_s) until the closure of the aortic valve (B_d). The systolic SCG variables were divided into three periods, respectively early systole from E_s to G_s, late systole from G_s to B_d, and the entire systole including overlapping time intervals, as seen in table 1. All periods included amplitudes, time intervals and peak to peak intervals. SCG data detection relies on the mean of multiple measurements of heartbeats for each subject during the same recording session.

Systolic echocardiographic variables

The included echo parameters indicative of the systolic function in this study are respectively; stroke volume (SV), left ventricular ejection fraction (LVEF), peak systolic velocity (S'), strain, strain rate (SR), left ventricular ejection time (LVET), isovolumetric contraction time (IVCT) and early ejection time (EET). EET is included as a relevant time interval of the systolic function, defined as the time from the opening of the aortic valve until the systolic peak velocity S'. The echo was performed and analyzed by an experienced echo specialist (P.S.) [18, 21, 23]. All the parameters mentioned above were assessed manually: LV volumes and LVEF by the echo-application Auto Ejection Fraction, strain and SR by speckle tracking, and the time intervals as well as S' by analyzing PW TDI. The echo parameters were detected through a single measurement for each parameter in all subjects.

Statistical analysis

All data were plotted as histograms and QQ-plots and tested for normality using the Sharpiro Wilk test. Furthermore, Levene's test of homogeneity was performed. A Pearson's Correlation Coefficient test or a Spearman's Rho Correlation Coefficient test was used to investigate the correlation between the systolic SCG and echo variables. Beforehand, scatter plots were performed to test for outliers.

A paired sample t-test or a paired sample Wilcoxon test was applied to test if SCG and echo variables were significantly affected by a decrease in preload. All statistical analyses were considered significant at $p < 0.05$ and the correlation coefficients were considered relevant at $r > 0.3$ or $r < -0,3$ [24]. The correlations had to be significant in both supine and tilted position to be considered relevant. The statistical analysis of this study was performed in IBM SPSS Statistics for Mac, version 28 (IBM Corp., Armonk, NY, USA).

Results

A total of 45 subjects were recruited. One subject withdrew in advance of the examination. In the collection of the SCG data, some of the fiducial points in the systole were not able to be determined in either the supine or tilted position due to limitations of the applied algorithm. Seven subjects were excluded, due to non-available SCG data in either supine or tilted position. Three subjects were excluded based on inconclusive echo data. In total 11 subjects were excluded, resulting in a total sample size of 34 subjects equally distributed between sex. The mean age was 45.4 years (±17.5), the mean height was 175.3 cm (±8.3), the mean weight was 74 kg (±12.7) and the mean BMI was 24 (±2.6).

The SCG data are for each subject based on the mean of heartbeats, detected by the algorithm. A boxplot illustrating the distribution of included heartbeats can be seen in Supplementary Material 2.

Changes in preload

The results of the paired samples test, comparing data of subjects in supine and tilted position, are

Table 2. The SCG variables and the difference between measurements of the supine- and tilted position.

Paired sample test of SCG-data in supine and tilted position										
	Supine			Tilted			Supine versus Tilted			
	Mean	SD	95% CI	Mean	SD	95% CI	Test	Mean Diff	SD	P-value
Time Intervals (ms)										
E_s to G_s	34.0	9.2	[30.8;37.2]	35.9	8.00	[33.0;38.6]	W	1.9	8.8	.149
E_s to K_s	87.6	16.4	[81.7;93.5]	97.6	16.9	[91.7;103.5]	T	10.0	13.3	.001*
E_s to L_s	126.5	17.2	[120.5;132.5]	134.4	17.6	[128.2;140.5]	W	7.9	15.9	.005*
E_s to F_s	10.9	3.8	[9.6;12.2]	12.1	6.0	[10.1;14.2]	W	1.2	5.7	.918
F_s to G_s	23.1	7.8	[20.4;25.8]	23.7	6.4	[21.4;25.9]	T	0.6	6.3	.595
F_s to K_s	76.7	15.6	[71.2;82.1]	85.4	15.2	[80.1;90.7]	W	8.7	11.6	.001*
F_s to L_s	115.6	15.7	[110.1;121.1]	122.2	15.8	[116.7;127.7]	W	6.6	12.5	.003*
G_s to K_s	53.6	15.2	[48.3;58.9]	61.7	15.5	[56.3;67.1]	T	8.1	10.0	.001*
G_s to L_s	92.5	14.5	[87.4;97.6]	98.5	15.9	[93.0;104.1]	T	6.0	11.9	.006*
K_s to L_s	37.9	9.7	[34.5;41.2]	36.9	10.6	[33.2;40.6]	W	−1.0	12.6	.871
E_s to B_d	326.3	24.6	[317.7;334.8]	309.3	32.5	[298.0;320.6]	W	−17.0	21.2	.001*
F_s to B_d	315.4	24.7	[306.8;324.0]	297.1	32.1	[285.9;308.3]	W	−18.3	21.7	.001*
G_s to B_d	291.4	25.4	[282.5;300.2]	273.4	34.5	[261.4;285.5]	T	−18	22.9	.001*
K_s to B_d	238.7	23.8	[230.4;247.0]	210.0	31.1	[199.1;220.9]	W	−28.7	24.4	.001*
L_s to B_d	199.7	26.3	[190.6;208.9]	177.0	36.2	[164.4;189.6]	W	−22.7	29.5	.001*
Amplitudes and Amplitude Intervals (g)										
G_s	.0202	.0139	[.0153;.025]	.0187	.0099	[.0153;.0222]	W	−.0015	.0086	.602
F_s	−.0254	.0142	[−.03;−.02]	−.0199	.0105	[−.024;−.016]	W	−.0055	.0077	.001*
K_s	−.0095	.0060	[−.012;−.007]	−.0097	.0056	[−.012;−.009]	T	.0002	.0047	.76
L_s	.0071	.0037	[.006;.008]	.0045	.0035	[.003;.006]	T	−.0026	.0035	.001*
B_d	.0002	.0018	[−.0005;.0008]	.0009	.0028	[−.0001;.002]	W	.0007	.0021	.039*
F_s to G_s	.0455	.0260	[.0364;.0546]	.0386	.0184	[.0322;.0451]	W	−.0069	.0141	.031*
G_s to K_s	.0292	.0184	[.0228;.0356]	.0284	.0134	[.0238;.0331]	W	−.0008	.0109	.98
L_s to K_s	.0165	.0081	[.0136;.0193]	.0142	.0078	[.0114;.0169	W	−.0022	.0067	.023*

W = Wilcoxon paired sample test, T = paired sample t-test, *p < 0.05 were considered significant.

Table 3. The echo variables and the difference between measurements of the supine- and tilted position.

Paired sample test for echo-data in supine and tilted position										
	Supine			Tilted			Supine versus Tilted			
	Mean	SD	95% CI	Mean	SD	95% CI	Test	Mean Diff	SD	P-value
IVCT (ms)	78.9	20.0	[71.9;85.8]	74.4	14.6	[69.3;79.5]	T	−4.5	18.2	.164
LVET (ms)	303.6	30.2	[293.1;314.2]	283.2	34.7	[271.8;295.3]	T	−20.5	44.5	.012*
S' (cm/s)	10.8	2.3	[10.0;11.6]	10.4	2.4	[9.6;11.2]	T	−.4	1.9	.194
SV (mL/beat)	60.4	18.8	[53.8;66.9]	52.6	17.1	[46.7;58.6]	T	−7.8	6.1	.001*
LVEF (%)	61.4	3.2	[60.3;62.5]	61.1	3.8	[59.8;62.4]	T	−.3	3.6	.671
EET (ms)	46.8	12.7	[42.4;51.3]	47.0	13.4	[42.3;51.7]	W	−.2	16.2	.549
Strain (%)	−16.9	2.8	[−17.8;−15.9]	−14.4	2.6	[−15.3;−13.5]	W	−2.4	2.8	.001*
SR (s^{-1})	−.883	.1841	[−.947;−.819]	−.866	.121	[−.909;−.824]	W	−.017	0.16	.203
HR (BPM)	66.5	11.9	[62.3;70.6]	67.5	10.5	[63.8;71.1]	T	1	8.8	.514

W = Wilcoxon paired sample test, T = paired sample t-test, *p < 0.05 were considered significant.

represented respectively in table 3 for echo measurements and table 2 for SCG measurements. LVET, SV, and strain, were able to detect a significant decrease in preload when tilting the subjects. Almost all the examined systolic SCG variables, were able to measure a change in preload, including variables from both the early, late, and entire systole. Six of the SCG time intervals are significantly increasing and five time intervals are significantly decreasing after a 30° head-up tilted position. The amplitude B_d increased significantly after the tilt, whereas the amplitudes F_s and L_s and the peak to peak intervals F_s-G_s and L_s-K_s are significantly decreased by tilting.

Correlation between SCG and echo

Correlations between the systolic variables from SCG and echo are illustrated in figure 3. Significant correlations are demonstrated between SCG time intervals, including both intervals of the early, the late and the entire systole, and the echo variable LVET and IVCT both in supine and tilted position. Also, IVCT shows correlations to SCG amplitudes in the early systole and

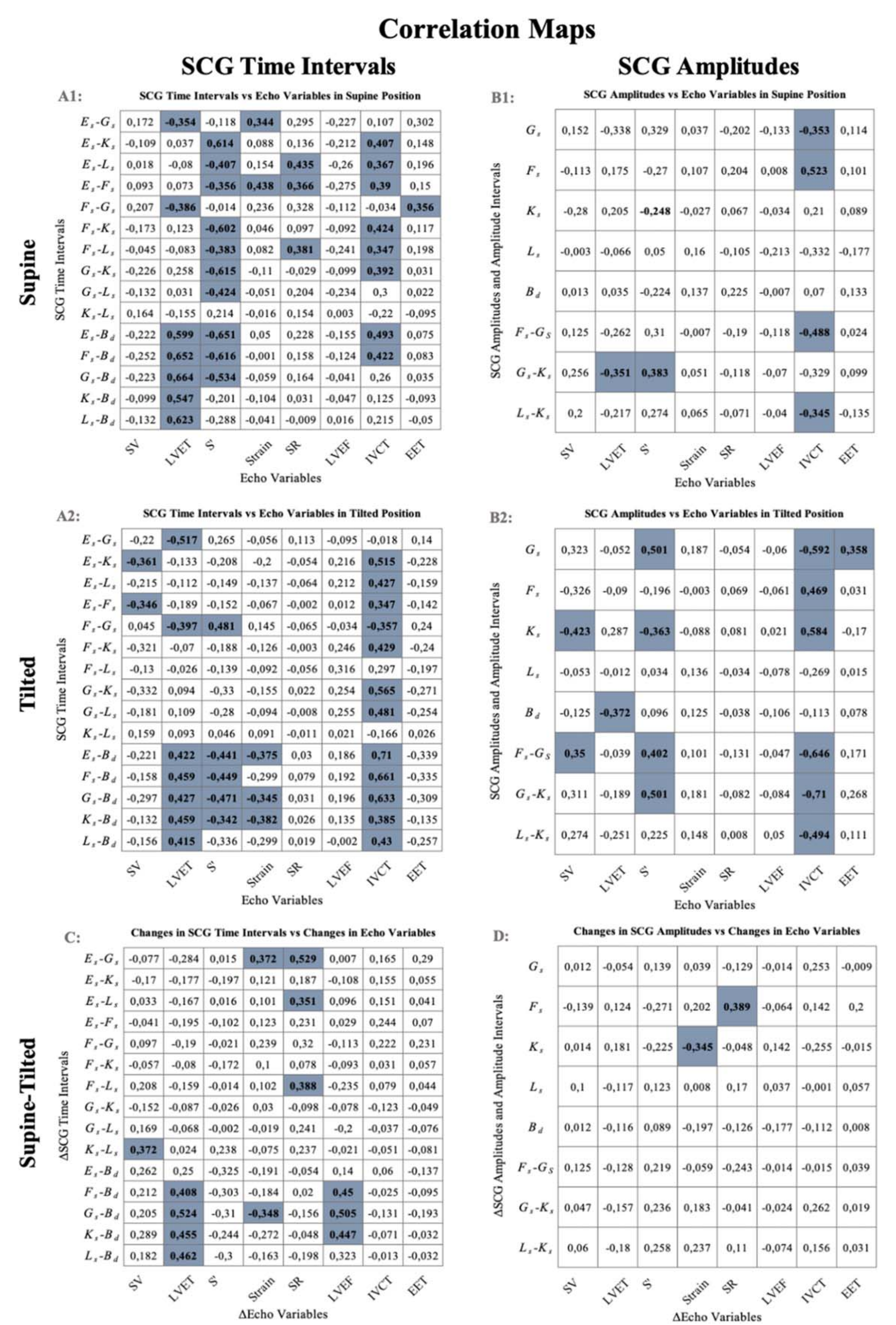

Correlation Maps

SCG Time Intervals

Supine

A1: SCG Time Intervals vs Echo Variables in Supine Position

SCG Time Intervals	SV	LVET	S'	Strain	SR	LVEF	IVCT	EET
E_s-G_s	0,172	**-0,354**	-0,118	**0,344**	0,295	-0,227	0,107	0,302
E_s-K_s	-0,109	0,037	**0,614**	0,088	0,136	-0,212	**0,407**	0,148
E_s-L_s	0,018	-0,08	**-0,407**	0,154	**0,435**	-0,26	**0,367**	0,196
E_s-F_s	0,093	0,073	**-0,356**	**0,438**	**0,366**	-0,275	**0,39**	0,15
F_s-G_s	0,207	**-0,386**	-0,014	0,236	0,328	-0,112	-0,034	**0,356**
F_s-K_s	-0,173	0,123	**-0,602**	0,046	0,097	-0,092	**0,424**	0,117
F_s-L_s	-0,045	-0,083	**-0,383**	0,082	**0,381**	-0,241	**0,347**	0,198
G_s-K_s	-0,226	0,258	**-0,615**	-0,11	-0,029	-0,099	**0,392**	0,031
G_s-L_s	-0,132	0,031	**-0,424**	-0,051	0,204	-0,234	0,3	0,022
K_s-L_s	0,164	-0,155	0,214	-0,016	0,154	0,003	-0,22	-0,095
E_s-B_d	-0,222	**0,599**	**-0,651**	0,05	0,228	-0,155	**0,493**	0,075
F_s-B_d	-0,252	**0,652**	**-0,616**	-0,001	0,158	-0,124	**0,422**	0,083
G_s-B_d	-0,223	**0,664**	**-0,534**	-0,059	0,164	-0,041	0,26	0,035
K_s-B_d	-0,099	**0,547**	-0,201	-0,104	0,031	-0,047	0,125	-0,093
L_s-B_d	-0,132	**0,623**	-0,288	-0,041	-0,009	0,016	0,215	-0,05

Echo Variables

Tilted

A2: SCG Time Intervals vs Echo Variables in Tilted Position

SCG Time Intervals	SV	LVET	S'	Strain	SR	LVEF	IVCT	EET
E_s-G_s	-0,22	**-0,517**	0,265	-0,056	0,113	-0,095	-0,018	0,14
E_s-K_s	**-0,361**	-0,133	-0,208	-0,2	-0,054	0,216	**0,515**	-0,228
E_s-L_s	-0,215	-0,112	-0,149	-0,137	-0,064	0,212	**0,427**	-0,159
E_s-F_s	**-0,346**	-0,189	-0,152	-0,067	-0,002	0,012	**0,347**	-0,142
F_s-G_s	0,045	**-0,397**	**0,481**	0,145	-0,065	-0,034	**-0,357**	0,24
F_s-K_s	-0,321	-0,07	-0,188	-0,126	-0,003	0,246	**0,429**	-0,24
F_s-L_s	-0,13	-0,026	-0,139	-0,092	-0,056	0,316	0,297	-0,197
G_s-K_s	-0,332	0,094	-0,33	-0,155	0,022	0,254	**0,565**	-0,271
G_s-L_s	-0,181	0,109	-0,28	-0,094	-0,008	0,255	**0,481**	-0,254
K_s-L_s	0,159	0,093	0,046	0,091	-0,011	0,021	-0,166	0,026
E_s-B_d	-0,221	**0,422**	**-0,441**	**-0,375**	0,03	0,186	**0,71**	-0,339
F_s-B_d	-0,158	**0,459**	**-0,449**	-0,299	0,079	0,192	**0,661**	-0,335
G_s-B_d	-0,297	**0,427**	**-0,471**	**-0,345**	0,031	0,196	**0,633**	-0,309
K_s-B_d	-0,132	**0,459**	**-0,342**	**-0,382**	0,026	0,135	**0,385**	-0,135
L_s-B_d	-0,156	**0,415**	-0,336	-0,299	0,019	-0,002	**0,43**	-0,257

Echo Variables

Supine-Tilted

C: Changes in SCG Time Intervals vs Changes in Echo Variables

ΔSCG Time Intervals	SV	LVET	S'	Strain	SR	LVEF	IVCT	EET
E_s-G_s	-0,077	-0,284	0,015	**0,372**	**0,529**	0,007	0,165	0,29
E_s-K_s	-0,17	-0,177	-0,197	0,121	0,187	-0,108	0,155	0,055
E_s-L_s	0,033	-0,167	0,016	0,101	**0,351**	0,096	0,151	0,041
E_s-F_s	-0,041	-0,195	-0,102	0,123	0,231	0,029	0,244	0,07
F_s-G_s	0,097	-0,19	-0,021	0,239	0,32	-0,113	0,222	0,231
F_s-K_s	-0,057	-0,08	-0,172	0,1	0,078	-0,093	0,031	0,057
F_s-L_s	0,208	-0,159	-0,014	0,102	**0,388**	-0,235	0,079	0,044
G_s-K_s	-0,152	-0,087	-0,026	0,03	-0,098	-0,078	-0,123	-0,049
G_s-L_s	0,169	-0,068	-0,002	-0,019	0,241	-0,2	-0,037	-0,076
K_s-L_s	**0,372**	0,024	0,238	-0,075	0,237	-0,021	-0,051	-0,081
E_s-B_d	0,262	0,25	-0,325	-0,191	-0,054	0,14	0,06	-0,137
F_s-B_d	0,212	**0,408**	-0,303	-0,184	0,02	**0,45**	-0,025	-0,095
G_s-B_d	0,205	**0,524**	-0,31	**-0,348**	-0,156	**0,505**	-0,131	-0,193
K_s-B_d	0,289	**0,455**	-0,244	-0,272	-0,048	**0,447**	-0,071	-0,032
L_s-B_d	0,182	**0,462**	-0,3	-0,163	-0,198	0,323	-0,013	-0,032

ΔEcho Variables

SCG Amplitudes

B1: SCG Amplitudes vs Echo Variables in Supine Position

SCG Amplitudes and Amplitude Intervals	SV	LVET	S'	Strain	SR	LVEF	IVCT	EET
G_s	0,152	-0,338	0,329	0,037	-0,202	-0,133	**-0,353**	0,114
F_s	-0,113	0,175	-0,27	0,107	0,204	0,008	**0,523**	0,101
K_s	-0,28	0,205	**-0,248**	-0,027	0,067	-0,034	0,21	0,089
L_s	-0,003	-0,066	0,05	0,16	-0,105	-0,213	-0,332	-0,177
B_d	0,013	0,035	-0,224	0,137	0,225	-0,007	0,07	0,133
F_s-G_S	0,125	-0,262	0,31	-0,007	-0,19	-0,118	**-0,488**	0,024
G_s-K_s	0,256	**-0,351**	**0,383**	0,051	-0,118	-0,07	-0,329	0,099
L_s-K_s	0,2	-0,217	0,274	0,065	-0,071	-0,04	**-0,345**	-0,135

Echo Variables

B2: SCG Amplitudes vs Echo Variables in Tilted Position

SCG Amplitudes and Amplitude Intervals	SV	LVET	S'	Strain	SR	LVEF	IVCT	EET
G_s	0,323	-0,052	**0,501**	0,187	-0,054	-0,06	**-0,592**	**0,358**
F_s	-0,326	-0,09	-0,196	-0,003	0,069	-0,061	**0,469**	0,031
K_s	**-0,423**	0,287	**-0,363**	-0,088	0,081	0,021	**0,584**	-0,17
L_s	-0,053	-0,012	0,034	0,136	-0,034	-0,078	-0,269	0,015
B_d	-0,125	**-0,372**	0,096	0,125	-0,038	-0,106	-0,113	0,078
F_s-G_S	**0,35**	-0,039	**0,402**	0,101	-0,131	-0,047	**-0,646**	0,171
G_s-K_s	0,311	-0,189	**0,501**	0,181	-0,082	-0,084	**-0,71**	0,268
L_s-K_s	0,274	-0,251	0,225	0,148	0,008	0,05	**-0,494**	0,111

Echo Variables

D: Changes in SCG Amplitudes vs Changes in Echo Variables

ΔSCG Amplitudes and Amplitude Intervals	SV	LVET	S'	Strain	SR	LVEF	IVCT	EET
G_s	0,012	-0,054	0,139	0,039	-0,129	-0,014	0,253	-0,009
F_s	-0,139	0,124	-0,271	0,202	**0,389**	-0,064	0,142	0,2
K_s	0,014	0,181	-0,225	**-0,345**	-0,048	0,142	-0,255	-0,015
L_s	0,1	-0,117	0,123	0,008	0,17	0,037	-0,001	0,057
B_d	0,012	-0,116	0,089	-0,197	-0,126	-0,177	-0,112	0,008
F_s-G_S	0,125	-0,128	0,219	-0,059	-0,243	-0,014	-0,015	0,039
G_s-K_s	0,047	-0,157	0,236	0,183	-0,041	-0,024	0,262	0,019
L_s-K_s	0,06	-0,18	0,258	0,237	0,11	-0,074	0,156	0,031

ΔEcho Variables

Figure 3. Correlation maps illustrating the correlation between the systolic SCG- and echo variables represented by either Pearson's Correlation Coefficient or Spearman's Rho Correlation Coefficient. The maps illustrate respectively supine-, tilted-, and the change between the positions. The coloured cells mark the correlations which are higher than $r > \pm 0.3$ and statistically significant ($p < 0.05$). Bold r-values are significant correlations ($p < 0.05$). Exact p-values are seen in Supplementary Material 1.

peak to peak intervals in both the early and late systole in both positions. Furthermore, significant correlations are seen between S' and wide SCG time intervals of respectively the late systole and the entire systole in both positions. S' also correlates low and moderate with the amplitudes of K_s and the peak to peakinterval G_s-K_s in both supine and tilted position.

The changes in supine and tilted positions of SV correlates with the changes in the SCG time interval K_s-L_s in the late systole. For the change in LVET, there are low and moderate correlations with the change in SCG time intervals in the entire and late systole. Regarding the change in strain, there are low correlations with the change in SCG time intervals of the late and early systole and with the change of the amplitude K_s in the late systole. Change in SR shows significant low and moderate correlations with the change in time intervals in the early and entire systole, and the amplitude F_s in the early systole. Regarding the change in LVEF, significant low and moderate correlations are detected in the comparison with the change in SCG time intervals in the entire and late systole. Correlation plots visualizing the correlations between selected SCG and echo variables are seen in figure 4.

Discussion

In this study, the systolic fiducial points were utilized, leading to an investigation of systolic SCG variables as well as systolic echocardiography variables. Thereby, an attempt is made to achieve a more comprehensive understanding of the correlation between SCG and echocardiography, as well as the sensitivity to preload changes in both assessment methods.

Changes in preload

Most of the SCG time intervals in the entire systole, as seen in table 2, exhibited a significant increase when decreasing preload. Particularly, the time intervals that initiate in the early systole (E_s-K_s, E_s-L_s, F_s-K_s, F_s -L_s) and end at the beginning of the late systole (G_s-K_s, G_s-L_s) are significantly prolonged, which which reflects a prolonged time to ejection [25]. In the late systole a shortening of the ejection period was expected [26]. This aligns with the results of a significant decrease of the late systole time intervals, as seen in table 2. The time intervals at the beginning of the late systole (G_s-B_d, K_s-B_d, L_s-B_d) were significantly increased. This could potentially be related to a prolonged contraction time required to achieve peak systolic outflow. All the significant altered amplitudes (F_s, L_s), except B_d, and all the significant altered peak to peakintervals (F_s-G_s, L_s-K_s), exhibit a significant decrease, as seen in table 2, which aligns with reduced contractility caused by the preload reduction [27].

A study by Shandhi *et al* [28] also confirms that SCG parameters are sensitive to preload reductions. However, Agam *et al* [19] found that only the diastolic amplitude E_d were significantly altered when decreasing the preload. This may indicate that more systolic variables are affected by changes in preload compared to the diastolic variables. Further investigation is highly relevant to confirm the sensitivity towards preload and enhance the understanding of SCG as a diagnostic tool. An increased preload is associated with various pathological conditions, such as heart failure, and therefore a preload detection tool is highly relevant [29].

As seen in table 3, regarding echo only LVET, SV and strain were significantly altered by a decrease in preload, even though various echo variables have shown to be sensitive towards preload changes [30, 31]. The results of this study indicate that systolic SCG variables are more sensitive to preload alterations than systolic echo variables. SCG could potentially be a diagnostic tool, for early discovery of pathological conditions with preload impacts, such as heart failure and fluid monitoring in patients with edema. Along with the easy manageability, this substantiates the potential of SCG as a future home monitoring device. On the other hand, the lack of affected echo variables could be because the 30° tilting may not generate a sufficient preload change. This study used the change from supine to 30° head-up tilted position to create changes in preload. This experimental design presumably creates a minor haemodynamic change compared to other methods. In other studies, different hemodynamic manoeuvres, such as lower body negative pressure as used in the study by Tavakolian *et al* [32], are applied to create changes in hemodynamic parameters. These manoeuvres would probably induce greater hemodynamic changes, which theoretically would induce more impact on the SCG-parameters. In future studies, it would be relevant to investigate the influence of SCG-parameters under greater changes in the haemodynamics, to support the theory of SCG's ability to detect these changes in preload.

Correlation between seismocardiography and echocardiography

LVET shows a correlation with several SCG time intervals as seen in figures 3(A1), (A2), including a moderate and a low correlation with the interval G_s-B_d, that corresponds to the definition of LVET [18, 33]. This correlation between SCG and LVET is also demonstrated in a study by Rienzo *et al* [34]. There is also demonstrated a moderately significant correlation between the change in G_s-B_d and the change in LVET, seen in figure 3(C), indicating sensitivity to a decrease in preload of both variables. It is suggested by the paired samples test in table 2 and table 3 and by the correlation in changes in figures 3(A1), (A2), (C), that SCG and LVET are able to detect a decrease in preload.

Regarding IVCT a significant correlation with the time interval E_s-F_s, in the early systole was

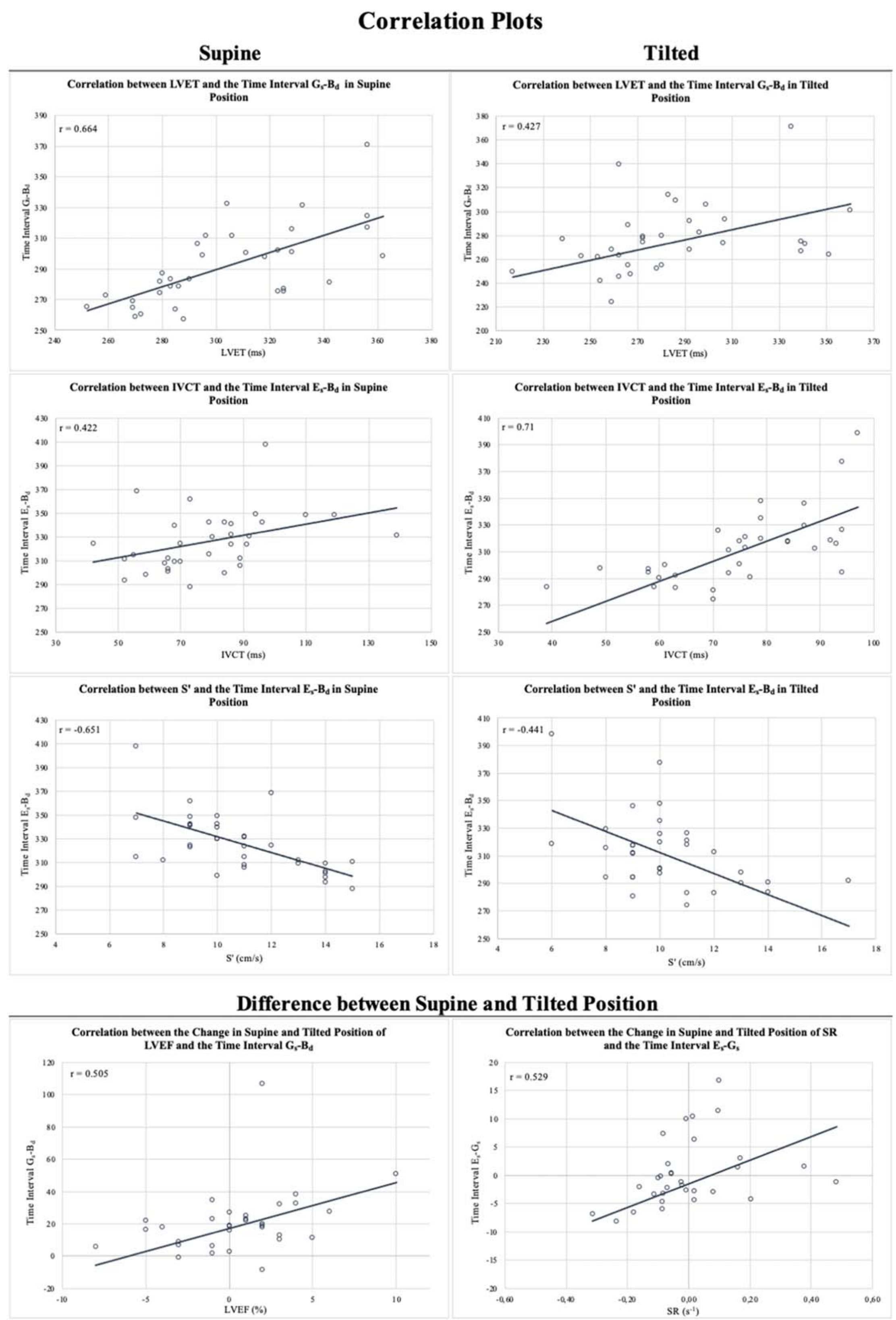

Figure 4. Correlation plots for certain SCG- and echo variables in respectively supine- and tilted position and the difference between the two positions.

demonstrated, as seen in figures 3(A1), (A2). This corresponds to the expected physiological appearance of IVCT. A significant low and moderate correlation was observed in the early systole, respectively to the amplitudes F_s and G_s, and to the peak to peak interval F_s-G_s. The negative correlation to G_s and F_s-G_s could indicate a lower acceleration results in prolonged IVCT. Further investigation into these parameters could be relevant, since IVCT is a relevant and informative parameter for the function of the heart. Understanding how IVCT relates to SCG, there is a potential to utilize SCG as a mean to offer diagnostic and prognostic information about the heart.

As seen in figures 3(A1), (A2), a significant moderate and low correlation has been demonstrated between S' and a SCG time interval (E_s-B_d), equalling the entire systole, which has a low correspondence. S' has also been demonstrated to correlate respectively low and moderate with the amplitude K_s and the peak to peak interval G_s-K_s in the late systole, as seen in figures 3(B1), (B2). S' likely occurs around these points in the cardiac cycle, which makes this area of the SCG interesting to further investigate. In the clinical use, S' can be useful in detecting patients with LV systolic dysfunction [35–37].

The changes in strain have a low correlation with the changes in the late amplitude K_s and the change of two SCG time intervals (E_s-G_s, G_s-B_d), representing respectively the early and the late systole, as seen in figures 3(C), (D). Further investigations are relevant regarding K_s and the systolic time intervals. On the other hand, no relevant correlations between strain in supine or tilted position and any of the fiducial points were found, as demonstrated in figures 3(A1), (A2), (B1), (B2). This indicates strain does not correspond to specific fiducial points but is still able to detect a change in preload in correlation with SCG variables, which also is supported by Grund *et al* [38] who suggested that strain correlates with preload. This is also supported by the paired sample test, seen in table 3, where strain significantly changed after tilting the subjects.

Change in SR shows moderate and low significant correlations with the change in time intervals in the early and entire systole (E_s-G_s = 0,529, E_s-L_s = 0,351, F_s-L_s = 0,388), as seen in figure 3(C). The highest correlation is seen to the change in the time interval E_s-G_s. Furthermore, the change in SR displays a low correlation to the amplitude F_s in the early systole, seen in figure 3(D). This indicates a possible correlation of changes in the early systole. Both strain and SR display the highest correlation to the time interval E_s-G_s, indicating the expected relation between these echo parameters [39].

A low significant correlation between the change in SCG time interval K_s-L_s (r = 0,372) and the change in SV was demonstrated, seen in figure 3(C). This would be a relevant correlation since the time interval approximately represents the time from the peak systolic outflow until the next positive deflection in the SCG curve [18, 40]. In addition, there were no significant correlations found between the SCG variables and SV. This indicates that SV cannot be estimated using single SCG fiducial points, but potentially it can be used to estimate the changes in SV.

The changes in LVEF significantly correlate low and moderately to the changes in one time interval of the entire systole (F_s-B_d, r = 0,45) and two late time intervals (G_s-B_d (r = 0,505), K_s-B_d (r = 0,447)), as seen in figure 3(C), which indicates that the SCG may be able to detect the changes in LVEF when decreasing preload. The time interval changes that correlated with LVEF changes are all represented in the periode from the closure of the mitral valve until the closure of the aortic valve, which is in physiological consistency with the occurence of blood ejection and thereby LVEF [18, 33]. The highest correlation is seen with the change of the late systolic time interval G_s-B_d. There were only correlations between the changes in the LVEF and the time interval G_s-B_d. Theoretically, LVEF should be affected by preload [31], but the echo data show no significant difference comparing supine and tilted position, as demonstrated in table 3. In this case, it could impair the basis of comparison.

Study limitations

A limitation of this study is the small number of included subjects. Furthermore, this study has an exploratory approach, and therefore requires further verification. The applications of the SCG as a measurement may be affected by confounders, such as skin impedance, BMI and sex, as demonstrated in a study by Sørensen *et al* [41]. It would be relevant in future studies to explore the influence of these potential confounders to enable appropriate adjustments. This study only included healthy subjects, which reduces the transferability of the results, to patients with cardiovascular diseases. The application and analysis of SCG remain challenging due to the lack of consensus on methods, analysis tools, and algorithms [12, 14, 42]. To gain more consensus Sørensen *et al* [18] attempted to make a general approach to SCG by defining fiducial points. In addition, inter-observer variability can occur in both the performance and the interpretation of echo [6]. Furthermore, the autonomic nervous system can possibly influence the results. In particular, the echo results that were obtains after the SCG recordings are at risk of being affected, as normalization of preload may occur before the transducer is placed.

Conclusion

SCG is able to detect a change in systolic variables when preload is decreased. Several moderate correlations are detected between systolic echo variables and selected systolic SCG variables. The findings in this study demonstrates the potential of SCG as a clinical supplement in the examination of the systolic mechanical function of the heart.

Data availability statement

All data that support the findings of this study are included within the article (and any supplementary files).

ORCID iDs

Christoffer Mejling Kolind https://orcid.org/0009-0000-9400-2389
Samuel Schmidt https://orcid.org/0000-0002-0917-634X

References

[1] World Health Organisation 2021 Cardiovascular diseases (CVDs) (https://who.int/news-room/fact-sheets/detail/cardiovascular-diseases-(cvds)
[2] Heidenreich P A *et al* 2011 Forecasting the future of cardiovascular disease in the United States: a policy statement from the american heart association *Circulation* **123** 933–44
[3] St. John Sutton M and Wiegers S E 2007 Echocardiography in heart failure: applications, utility, and new horizons *J. Am. Coll. Cardiol.* **50** 381–96
[4] Reichlin T *et al* 2016 Advanced ECG in 2016: is there more than just a tracing? *Swiss Med. Wkly [Internet]* **146** 1718
[5] Salustri A and Trambiaolo P 2003 The 'ultrasonic stethoscope': is it of clinical value? *Heart Journal* **89** 704–6
[6] Vignola P A, Bloch A, Kaplan A D, Walker H J, Chiotellis P N and Myers G S 1977 Interobserver variability in echocardiography *J. Clin. Ultrasound* **5** 238–42
[7] Roth G A *et al* 2020 Global burden of cardiovascular diseases and risk factors, 1990-2019: update from the GBD 2019 study *J. Am. Coll. Cardiol* **76** 2982–3021
[8] Flower L, Dempsey M, White A, Sanfilippo F, Olusanya O and Madhivathanan P R 2021 Training and accreditation pathways in critical care and perioperative echocardiography *J. Cardiothorac Vasc Anesth* **35** 235–47
[9] Therming C *et al* 2018 Low diagnostic yield of non-invasive testing in patients with suspected coronary artery disease: results from a large unselected hospital-based sample *Eur. Heart J. Qual. Care Clin. Outcomes* **4** 301–8
[10] Di Rienzo M *et al* 2011 A wearable system for the seismocardiogram assessment in daily life conditions *Annu. Int. Conf. IEEE Eng. Med. Biol. Soc.* **2011** 4263–6 (https://pubmed.ncbi.nlm.nih.gov/22255281/)
[11] Mounsey P 1956 PRÆCORDIAL BALLISTOCARDIOGRAPHY *Heart Journal* **19** 259–271
[12] Taebi A, Solar B E, Bomar A J, Sandler R H and Mansy H A 2019 Recent advances in seismocardiography *Vibration* **2** 64–86
[13] Munck K, Sorensen K, Struijk J J and Schmidt S E 2020 Multichannel seismocardiography: an imaging modality for investigating heart vibrations *Physiol Meas* **41** 115001
[14] Ashouri H, Hersek S and Inan O T 2018 Universal pre-ejection period estimation using seismocardiography: quantifying the effects of sensor placement and regression algorithms *IEEE Sens J.* **18** 1665
[15] Johnson E M I, Etemadi M, Malaisrie S C, McCarthy P M, Markl M and Barker A J 2020 Seismocardiography and 4D flow MRI reveal impact of aortic valve replacement on chest acceleration and aortic hemodynamics *J. Card. Surg.* **35** 232–5
[16] Ganti V G *et al* 2022 Wearable seismocardiography-based assessment of stroke volume in congenital heart disease *Journal of the American Heart Association: Cardiovascular and Cerebrovascular Disease* **11** 26067
[17] Kumar Jain P, Kumar Tiwari A and Chourasia V S 2016 Performance analysis of seismocardiography for heart sound signal recording in noisy scenarios *J. Med. Eng. Technol.* **40** 106–18
[18] Sørensen K, Schmidt S E, Jensen A S, Søgaard P and Struijk J J 2018 Definition of fiducial points in the normal seismocardiogram *Sci. Rep.* **8** 1–11
[19] Agam A *et al* 2022 Correlation between diastolic seismocardiography variables and echocardiography variables *Eur. Heart J. - Digital Health* **3** 465–72
[20] Klaeboe L G and Edvardsen T 2019 Echocardiographic assessment of left ventricular systolic function *J. Echocardiogr* **17** 10–6
[21] Mogelvang R, Sogaard P, Pedersen S A, Olsen N T, Schnohr P and Jensen J S 2009 Tissue doppler echocardiography in persons with hypertension, diabetes, or ischaemic heart disease: the copenhagen city heart study *Eur. Heart J.* **30** 731–9
[22] Schmidt S E, Holst-Hansen C, Graff C, Toft E and Struijk J J 2010 Segmentation of heart sound recordings by a duration-dependent hidden Markov model *Physiol. Meas.* **31** 513–29
[23] Hoffmann S *et al* 2011 Tissue Doppler echocardiography reveals impaired cardiac function in patients with reversible ischaemia *Eur. J. Echocardiogr.* **12** 628–34
[24] Mukaka M M 2012 A guide to appropriate use of Correlation coefficient in medical research *Malawi. Med. J.* **24** 69 (/pmc/articles/PMC3576830/)
[25] Khanna P K, Shah P M, Kramer D H, Schaefer R A and Tager I 1973 Effects of altered preload on left ventricular systolic time intervals in acute myocardial infarction *Br. Heart J.* **973** 2–08
[26] Alhakak A S, Teerlink J R, Lindenfeld J, Böhm M, Rosano G M C and Biering-Sørensen T 2021 The significance of left ventricular ejection time in heart failure with reduced ejection fraction *Eur. J. Heart Fail* **23** 541–51
[27] Weyland A and Grüne F 2009 Cardiac preload and central venous pressure *Anaesthesist* **58** 506–12
[28] Hasan Shandhi M M *et al* 2020 Cardiac function monitoring for patients undergoing cancer treatments using wearable seismocardiography: a proof-of-concept study *Annu. Int. Conf. IEEE Eng. Med. Biol. Soc.* **2020** 4075–8 (https://pubmed.ncbi.nlm.nih.gov/33018894/)
[29] O'Keefe E and Singh P 2022 Physiology, cardiac preload StatPearls (https://ncbi.nlm.nih.gov/books/NBK541109/)
[30] Pelà G *et al* 2004 Effects of the reduction of preload on left and right ventricular myocardial velocities analyzed by Doppler tissue echocardiography in healthy subjects *European Journal of Echocardiography* **5** 262–71
[31] Delicce A V and Makaryus A N 2023 Physiology, frank starling law StatPearls (https://ncbi.nlm.nih.gov/books/NBK470295/)
[32] Tavakolian K, Dumont G A, Houlton G and Blaber A P 2014 Precordial vibrations provide noninvasive detection of early-stage hemorrhage *Shock* **41** 91–6
[33] Biering-Sørensen T *et al* 2018 Left ventricular ejection time is an independent predictor of incident heart failure in a community based cohort *Eur. J. Heart Fail* **20** 1106
[34] Di Rienzo M, Vaini E, Castiglioni P, Meriggi P and Rizzo F 2013 Beat-to-beat estimation of LVET and QS2 indices of cardiac mechanics from wearable seismocardiography in ambulant subjects *Proc. of the Annual Int. Conf. of the IEEE Engineering in Medicine and Biology Society* (EMBS) 7017–20
[35] Park Y S *et al* 2010 Usefulness of mitral annular systolic velocity in the detection of left ventricular systolic dysfunction: comparison with three dimensional echocardiographic data *J. Cardiovasc Ultrasound* **18** 1
[36] Ho C Y and Solomon S D 2006 *A Clinician's Guide to Tissue Doppler Imaging* vol 113 (Circulation)
[37] Pollock J D and Makaryus A N 2022 Physiology, cardiac cycle StatPearls (https://ncbi.nlm.nih.gov/books/NBK459327/)
[38] Grund F F, Kristensen C B, Myhr K A, Vejlstrup N, Hassager C and Mogelvang R 2021 Layer-specific strain is preload dependent: comparison between speckle-tracking echocardiography and cardiac magnetic resonance feature-tracking *J. Am. Soc. Echocardiogr.* **34** 377–87
[39] Pizzino F *et al* 2014 Diagnosis of chemotherapy-induced cardiotoxicity *J. Patient Cent. Res. Rev.* **1** 121–7
[40] Bruss Z S and Raja A 2022 Physiology, stroke volume StatPearls (https://ncbi.nlm.nih.gov/books/NBK547686/)
[41] Sorensen K, Poulsen M K, Karbing D S, Sogaard P, Struijk J J and Schmidt S E 2020 A clinical method for estimation of VO2max using seismocardiography *Int. J. Sports Med.* **41** 661–8
[42] Inan O T *et al* 2015 Ballistocardiography and seismocardiography: a review of recent advances *IEEE J. Biomed Health Inform* **19** 1414–27